

A water-stable zwitterionic dysprosium carboxylate metal organic framework: a sensing platform for Ebolavirus RNA sequences†

Liang Qin, Li-Xian Lin, Zhi-Ping Fang, Shui-Ping Yang, Gui-Hua Qiu, Jin-Xiang Chen,* and Wen-Hua Chen*

General.....	2
Synthesis of $\{[\text{Dy}(\text{Cm}(\text{dcp})(\text{H}_2\text{O})_3](\text{NO}_3)_2 \cdot 2\text{H}_2\text{O}\}_n$ (1).....	3
X-ray crystallography for compound 1	3
Detection of Ebolavirus RNA sequences.....	3
Measurement of fluorescence anisotropy.....	4
Table S1 Crystallographic data for 1	5
Table S2 Selected bond distances (Å) and angles (°) for compound 1	6
Fig. S1 Thermogravimetric analysis of compound 1	7
Fig. S2 3D structure of 1 as viewed down the <i>c</i> axis. All the hydrogen atoms are omitted for clarity. Color codes: Dy teal, O red, N blue, C black.....	7
Fig. S3 Fluorescence quenching efficiency of P-DNA (50 nM) by compound 1 , $\text{H}_3\text{Cm}(\text{dcp})\text{Br}$ and $\text{Dy}(\text{NO}_3)_3$ of varying concentrations in 100 nM Tris-HCl buffer (pH 7.4) at room temperature.....	8
Fig. S4 Fluorescence intensity of P-DNA@ 1 system (50 nM/11 μM) in the presence of T_0 (25 nM) in 100 nM Tris-HCl buffer (pH 7.4) at varying incubation time. Insets: plots of the fluorescence intensity at 518 nm <i>versus</i> the incubation time for T_0	8
Fig. S5 Fluorescence spectra of the P-DNA@ $\text{Dy}(\text{NO}_3)_3$ system (50 nM/32 μM) incubated with T_0 of varying concentrations in 100 nM Tris-HCl buffer (pH 7.4) at room temperature. Insets: plot of the fluorescence intensity at 518 nm <i>versus</i> the concentrations of T_0	9
Fig. S6 Fluorescence recovery efficiency (518 nm) of P-DNA@ 1 system (50 nM/11 μM) by T_0 , T_1 and T_2 of varying concentrations in 100 nM Tris-HCl buffer (pH 7.4).....	9
Fig. S7 Fluorescence spectra of P-DNA (50 nM) incubated with compound 1 of varying concentrations in 100 nM Tris-HCl buffer (pH 6.4) at room temperature. Inset: plot of the fluorescence intensity at 518 nm <i>versus</i> the concentrations of compound 1	10
Fig. S8 Fluorescence spectra of the P-DNA@ 1 system (50 nM/8 μM) incubated with T_0 of varying concentrations in 100 nM Tris-HCl buffer (pH 6.4) at room temperature. Insets: plot of the fluorescence intensity at 518 nm <i>versus</i> the concentrations of T_0	10
Fig. S9 Fluorescence recovery efficiency (518 nm) of P-DNA@ 1 system (50 nM/8 μM) by T_0 , T_1 and T_2 of varying concentrations in 100 nM Tris-HCl buffer (pH 6.4).....	11
Fig. S10 Fluorescence spectra of P-DNA (50 nM) incubated with compound 1 of varying concentrations in 100 nM Tris-HCl buffer (pH 8.0) at room temperature. Inset: plot of the fluorescence intensity at 518 nm <i>versus</i> the concentrations of compound 1	11
Fig. S11 Fluorescence spectra of the P-DNA@ 1 system (50 nM/13 μM) incubated with T_0 of varying concentrations in 100 nM Tris-HCl buffer (pH 8.0) at room temperature. Insets: plot of	

the fluorescence intensity at 518 nm versus the concentrations of T₀.....12

Fig. S12 Fluorescence recovery efficiency (518 nm) of P-DNA@1 system (50 nM/13 μM) by T₀, T₁ and T₂ of varying concentrations in 100 nM Tris-HCl buffer (pH 8.0) 12

General

IR spectra were recorded on a Nicolet MagNa-IR 550 infrared spectrometer. Elemental analyses for C, H, and N were performed on an EA1110 CHNS elemental analyzer. Thermogravimetric analysis (TGA) was performed on a SDTA851 Thermogravimetric Analyzer at a heating rate of 10 °C min⁻¹ under a nitrogen gas flow in an Al₂O₃ pan. Powder X-ray diffraction (PXRD) spectra were recorded with a Rigaku D/max-2200/PC. The X-ray generated from a sealed Cu tube was monochromated by a graphite crystal and collimated by a 0.5 mm MONOCAP (λ Cu-Kα = 1.54178 Å). The tube voltage and current were 40 kV and 40 mA, respectively. Fluorescence spectra and fluorescence anisotropy were measured on an LS55 spectrofluorimeter. Zeta potential measurement was carried out on a NanoZS90 zetasizer.

The DNA sequences were purchased from Sangon Inc. (Shanghai, China) and are shown below.

P-DNA: FAM-5'-CATGTGTCCAGCTGATTGCC-3'

The RNA sequences were purchased from TaKaRa. (Dalian, China) and are shown below:

Target RNA T₀: 5'-GGCA^AAUCAGUUGGACACAUG-3'

One base pair mutated for complementary target RNA T₁:

5'-GGCC^CAUCAGUUGGACACAUG-3'

Non-specific RNA T₂: 5'- GACCAACGTUUAGTCTCAUG-3'

All the samples were dissolved in 100 nM Tris-HCl buffer solution (pH 6.4, 7.4 or 8.0, 100 mM NaCl, 5 mM MgCl₂). DNA was stored at 4 °C and RNA was stored at -80 °C for use.

All the other reagents and solvents were obtained from commercial sources and used without further purification. All the instruments used for the detection of Ebolavirus RNA sequences were sterilized in an autoclavable container.

Synthesis of $\{[\text{Dy}(\text{Cmdcp})(\text{H}_2\text{O})_3](\text{NO}_3)_2\}_n$ (**1**)

A solution of $\text{H}_3\text{CmdcpBr}$ (37 mg, 0.12 mmol) in H_2O (5 mL) was adjusted to pH 6.0 with 0.1 M NaOH solution. Then, a solution of $\text{Dy}(\text{NO}_3)_3 \cdot 6\text{H}_2\text{O}$ (36 mg, 0.08 mmol) in H_2O (1 mL) was added. The clear, colorless solution was stirred for 0.5 h and then allowed to stand at room temperature for one week. The formed colorless crystals were collected by filtration and dried in vacuum to afford compound **1** (38 mg, 88%). Anal. Calcd. for $\text{C}_9\text{H}_{15}\text{DyN}_2\text{O}_{14} \cdot \text{H}_2\text{O}$: C 20.08, H 2.52, N 5.39. Found: C 20.13, H 2.46, N 5.31. Main IR bands (KBr disc, cm^{-1}) ν 3423 (s), 1647 (s), 1382 (s), 1237 (m), 1173 (w), 770 (m), 726 (m), 605 (m), 517 (m).

X-ray crystallography for compound **1**

All the measurements were made on a Bruker AXS APEX II diffractometer by using graphite-monochromated Mo $K\alpha$ ($\lambda = 0.71073 \text{ \AA}$). The data were subjected for empirical absorption correction using SADABS. All the crystal structures were solved by direct methods and refined on F^2 by full-matrix least-squares techniques with SHELXTL-97 program. The location of the two hydrogen atoms on the coordinated and free water were suggested by Calc-OH program in WinGX suite, and the water molecules were subsequently refined as rigid groups with $\text{O-H} = 0.85 \text{ \AA}$ and thermal parameters constrained to $U_{\text{iso}}(\text{H}) = 1.2U_{\text{eq}}(\text{O})$. The key crystallographic information for compound **1** was tabulated in Table S1.

Detection of Ebola virus RNA sequences

The fluorescence measurements were performed at room temperature. The fluorescence intensity at 518 nm with excitation at 480 nm was used for quantitative analysis (ex 480 nm, ex/em 10.0 nm/10.0 nm).

Firstly, fluorescence quenching experiments of P-DNA by compound **1**, $\text{H}_3\text{CmdcpBr}$ and $\text{Dy}(\text{NO}_3)_3$ were performed by keeping the concentrations of P-DNA constant, while gradually increasing the concentrations of each compound. Specifically, to a solution of P-DNA (50 nM) in 100 nM Tris-HCl (100 mM NaCl, 5 mM MgCl_2) were added aliquots of a solution of each compound containing P-DNA (50 nM) in the same buffer and oscillated. The corresponding fluorescence spectra were measured until saturation was observed. The quenching efficiency (Q_E , %) was

calculated according to Eq. (1).

$$Q_E\% = (1-F_M/F_0)\times 100\% \quad (1)$$

Wherein F_M and F_0 are the fluorescent intensities at 518 nm in the presence and absence of each compound, respectively.

Secondly, fluorescence recovery experiments were conducted by adding target RNA sequences of varying concentrations to the above saturated P-DNA@compound solution at room temperature, and the oscillation time was 120 min for each concentration until saturation of fluorescence recovery was observed. Fluorescence recovery efficiency was calculated according to Eq. (2).

$$R_E = F_T/F_M - 1 \quad (2)$$

Wherein F_T and F_M are the fluorescent intensities at 518 nm in the presence and the absence of target RNA, respectively.

Measurement of Fluorescence anisotropy

The fluorescence anisotropy changes of P-DNA (P, 50 nM) in the presence of compound **1**, T_0 (50 nM), or a mixture of T_0 (50 nM) and compound **1**, respectively, were measured at room temperature in 100 nM Tris-HCl solution. The emission intensity at 518 nm was recorded under the excitation at 480 nm. The incubation time for each mixture was 120 min.

Table S1 Crystallographic data for **1**

Molecular formula	C ₉ H ₁₅ DyN ₂ O ₁₄	D_{calc} (g cm ⁻³)	2.227
Formula weight	537.7	λ (Mo-K α) (Å)	0.71073
Crystal system	monoclinic	μ (cm ⁻¹)	4.741
Space group	<i>P2(1)/n</i>	Total reflections	16654
a (Å)	10.1045(5)	Unique reflections	3271
b (Å)	15.4994(7)	No. Observations	3134
c (Å)	10.4754(5)	No. Parameters	220
α (°)	90	R^a	0.0196
β (°)	102.2070(5)	wR^b	0.0512
γ (°)	90	GOF ^c	1.021
V (Å ³)	1603.50(13)	$\Delta\rho_{\text{max}}$ (e Å ⁻³)	2.898
Z	4	$\Delta\rho_{\text{min}}$ (e Å ⁻³)	-0.850
T/K	291(2)		

^a $R_1 = \Sigma||F_o| - |F_c|| / \Sigma|F_o|$. ^b $wR_2 = \{\Sigma[w(F_o^2 - F_c^2)^2] / \Sigma[w(F_o^2)^2]\}^{1/2}$. ^c $\text{GOF} = \{\Sigma[w(F_o^2 - F_c^2)^2] / (n-p)\}^{1/2}$, where n is the number of reflections and p is total number of parameters refined.

Table S2. Selected bond distances (Å) and angles (°) for compound **1**.

Gd(1)-O(2)#1	2.359(3)	Gd(1)-O(3W)	2.477(3)
Gd(1)-O(1)#2	2.371(3)	Gd(1)-O(2W)	2.488(3)
Gd(1)-O(6)	2.384(3)	Gd(1)-O(3)#4	2.537(3)
Gd(1)-O(5)#3	2.405(3)	Gd(1)-O(4)#4	2.561(3)
Gd(1)-O(1W)	2.453(3)		
O(2)#1-Gd(1)-O(1)#2	117.16(11)	O(5)#3-Gd(1)-O(2W)	73.13(11)
O(2)#1-Gd(1)-O(6)	74.84(11)	O(1W)-Gd(1)-O(2W)	81.35(11)
O(1)#2-Gd(1)-O(6)	74.62(11)	O(3W)-Gd(1)-O(2W)	131.09(10)
O(2)#1-Gd(1)-O(5)#3	72.40(11)	O(2)#1-Gd(1)-O(3)#4	141.88(11)
O(1)#2-Gd(1)-O(5)#3	76.61(11)	O(1)#2-Gd(1)-O(3)#4	76.54(10)
O(6)-Gd(1)-O(5)#3	118.80(11)	O(6)-Gd(1)-O(3)#4	75.44(10)
O(2)#1-Gd(1)-O(1W)	74.49(11)	O(5)#3-Gd(1)-O(3)#4	144.32(11)
O(1)#2-Gd(1)-O(1W)	140.51(11)	O(1W)-Gd(1)-O(3)#4	118.96(10)
O(6)-Gd(1)-O(1W)	142.03(11)	O(3W)-Gd(1)-O(3)#4	76.18(11)
O(5)#3-Gd(1)-O(1W)	71.53(11)	O(2W)-Gd(1)-O(3)#4	75.08(11)
O(2)#1-Gd(1)-O(3W)	71.71(11)	O(2)#1-Gd(1)-O(4)#4	126.58(10)
O(1)#2-Gd(1)-O(3W)	139.85(11)	O(1)#2-Gd(1)-O(4)#4	116.07(10)
O(6)-Gd(1)-O(3W)	70.38(11)	O(6)-Gd(1)-O(4)#4	115.97(11)
O(5)#3-Gd(1)-O(3W)	138.35(11)	O(5)#3-Gd(1)-O(4)#4	125.14(11)
O(1W)-Gd(1)-O(3W)	79.11(11)	O(1W)-Gd(1)-O(4)#4	67.77(10)
O(2)#1-Gd(1)-O(2W)	142.64(11)	O(3W)-Gd(1)-O(4)#4	65.26(11)
O(1)#2-Gd(1)-O(2W)	67.35(11)	O(2W)-Gd(1)-O(4)#4	65.86(11)
O(6)-Gd(1)-O(2W)	136.08(11)	O(3)#4-Gd(1)-O(4)#4	51.20(9)

Symmetry transformations used to generate equivalent atoms: #1 $-x + 1/2, y - 1/2, -z + 3/2$; #2 $x + 1/2, -y + 1/2, z + 1/2$; #3 $-x + 1, -y, -z + 2$; #4 $x, y, z + 1$; #5 $x - 1/2, -y + 1/2, z - 1/2$; #6 $-x + 1/2, y + 1/2, -z + 3/2$; #7 $x, y, z - 1$.

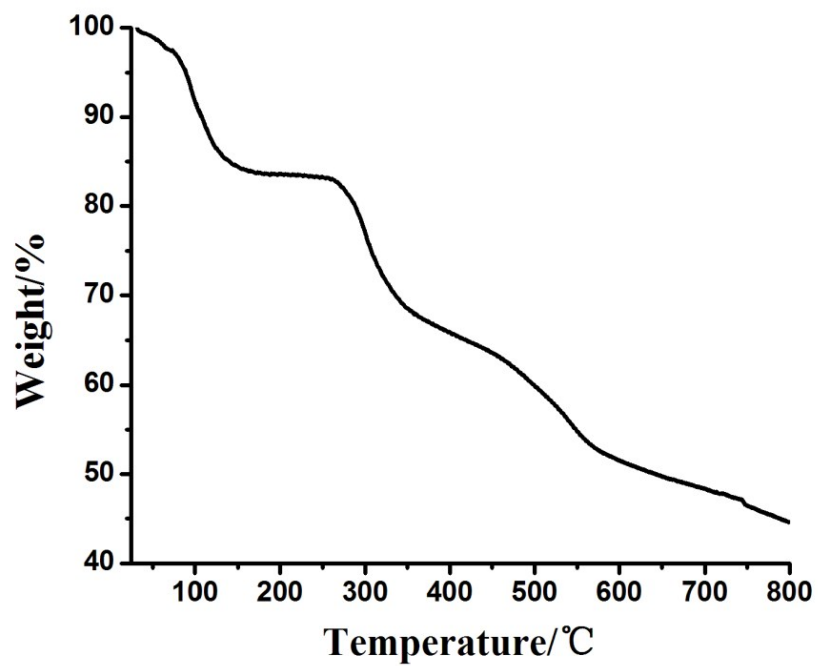


Fig. S1 Thermogravimetric analysis of compound **1**.

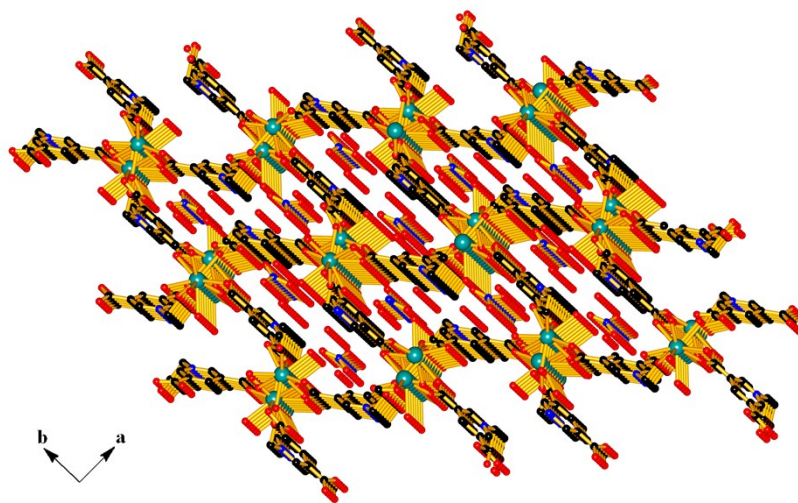


Fig. S2 3D structure of **1** viewed down the *c* axis. All the hydrogen atoms are omitted for clarity. Color codes: Dy teal, O red, N blue, C black.

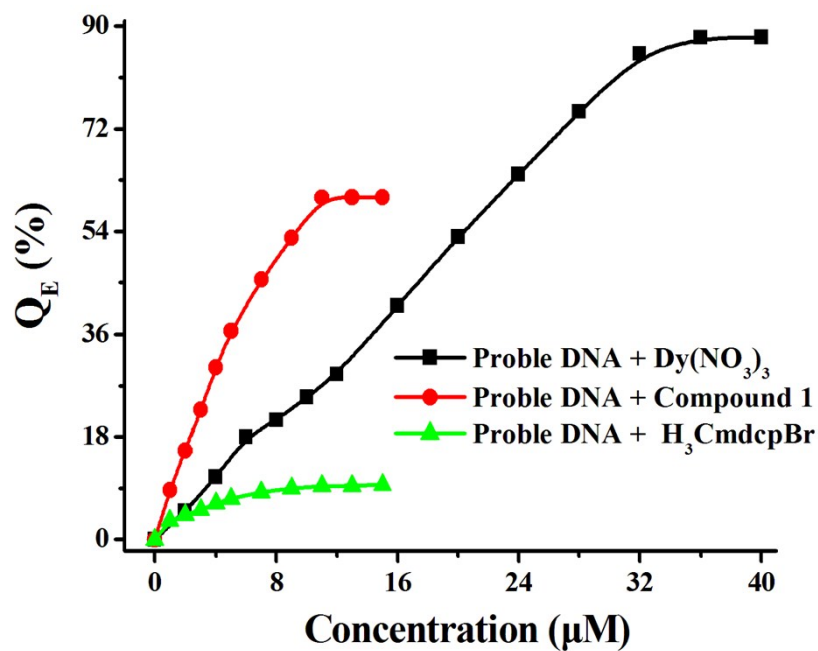


Fig. S3 Fluorescence quenching efficiency of P-DNA (50 nM) by compound 1, H₃CmcpBr and Dy(NO₃)₃ of varying concentrations in 100 nM Tris-HCl buffer (pH 7.4) at room temperature.

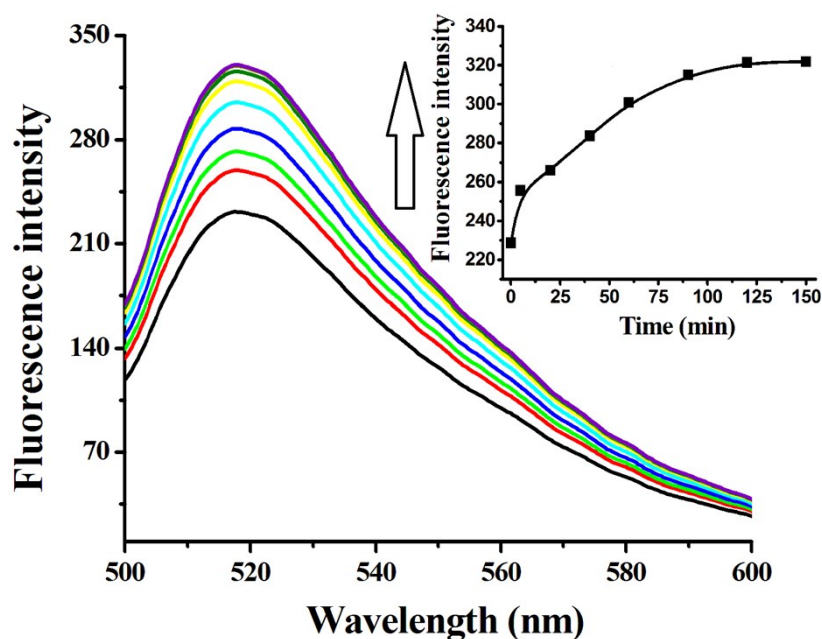


Fig. S4 Fluorescence intensity of P-DNA@1 system (50 nM/11 μM) in the presence of T₀ (25 nM) in 100 nM Tris-HCl buffer (pH 7.4) at varying incubation time. Inset: plot of the fluorescence intensity at 518 nm *versus* the incubation time for T₀.

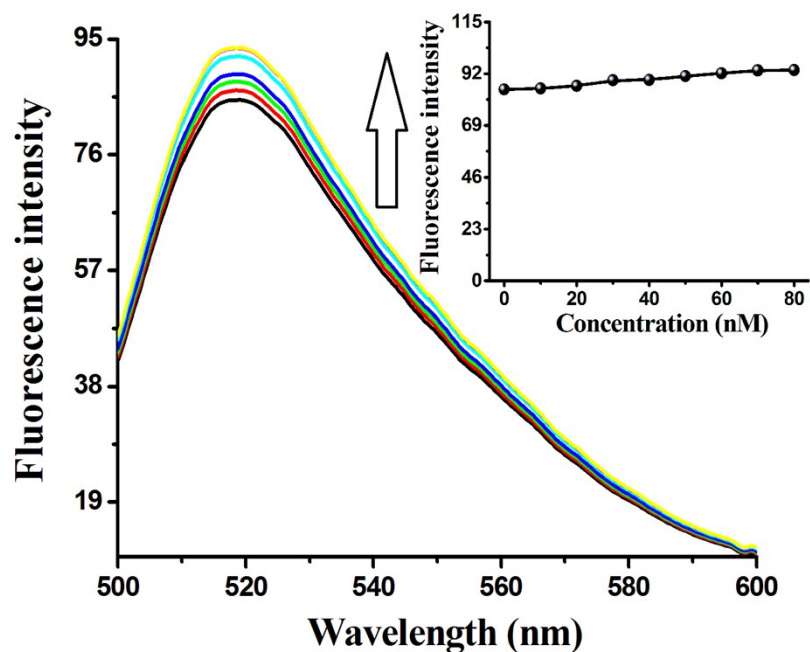


Fig. S5 Fluorescence spectra of the P-DNA@Dy(NO₃)₃ system (50 nM/32 μM) incubated with T₀ of varying concentrations in 100 nM Tris-HCl buffer (pH 7.4) at room temperature. Inset: plot of the fluorescence intensity at 518 nm *versus* the concentrations of T₀.

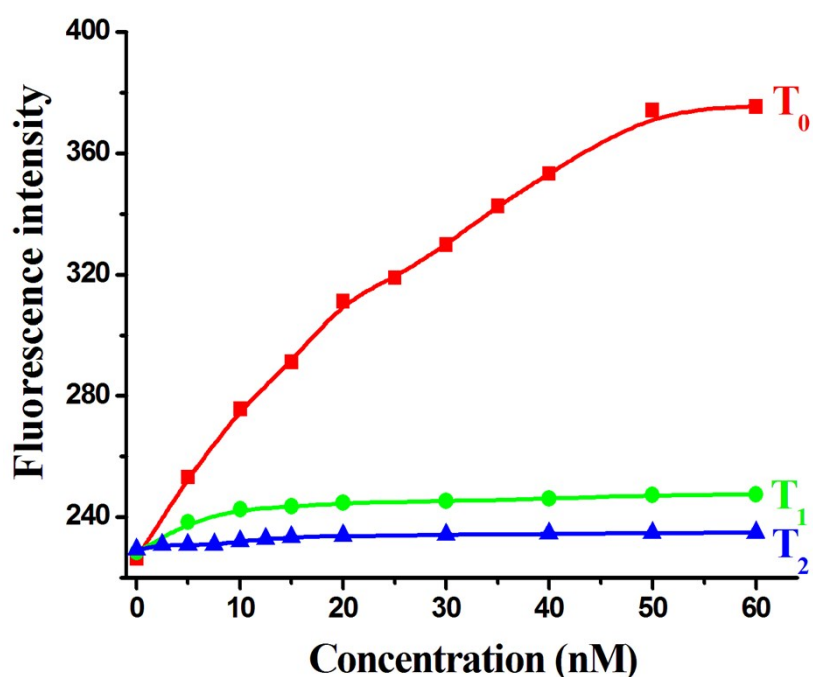


Fig. S6 Fluorescence recovery efficiency (518 nm) of P-DNA@1 system (50 nM/11 μM) by T₀, T₁ and T₂ of varying concentrations in 100 nM Tris-HCl buffer (pH 7.4).

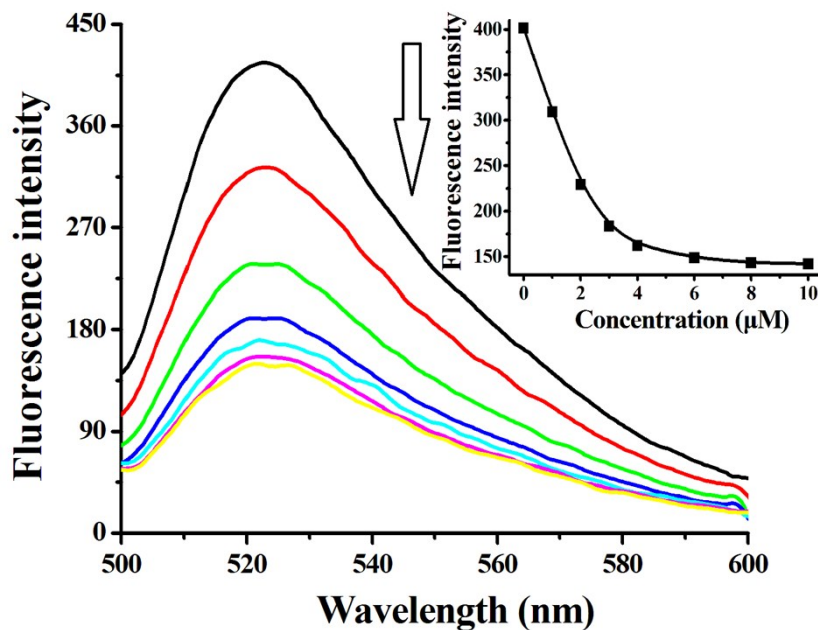


Fig. S7 Fluorescence spectra of P-DNA (50 nM) incubated with compound **1** of varying concentrations in 100 nM Tris-HCl buffer (pH 6.4) at room temperature. Inset: plot of the fluorescence intensity at 518 nm *versus* the concentrations of compound **1**.

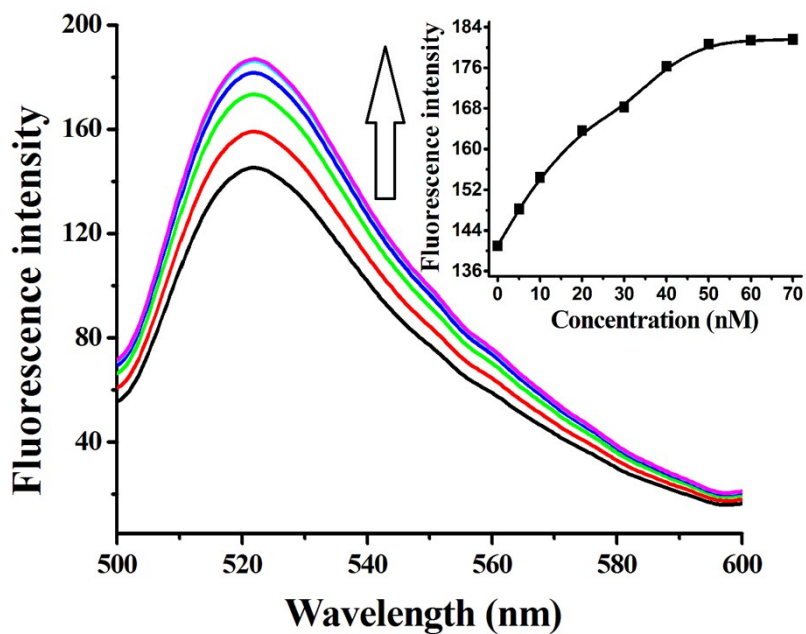


Fig. S8 Fluorescence spectra of the P-DNA@**1** system (50 nM/8 μM) incubated with T₀ of varying concentrations in 100 nM Tris-HCl buffer (pH 6.4) at room temperature. Inset: plot of the fluorescence intensity at 518 nm *versus* the concentrations of T₀.

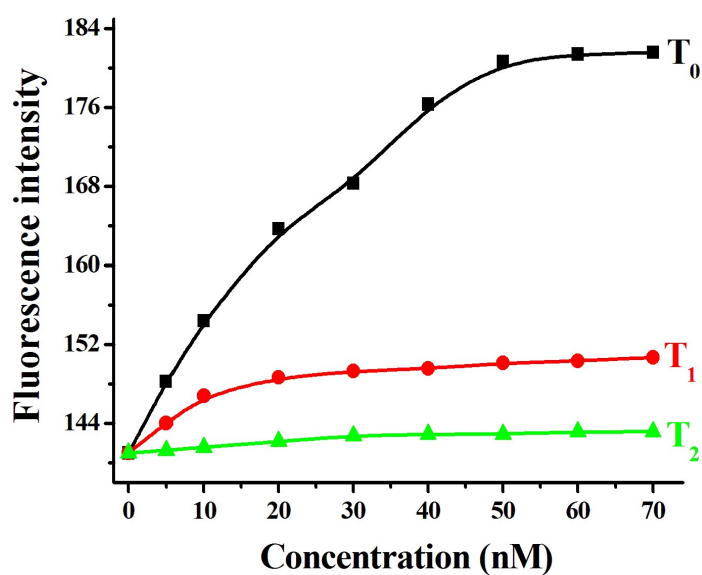


Fig. S9 Fluorescence recovery efficiency (518 nm) of P-DNA@**1** system (50 nM/8 μ M) by T₀, T₁ and T₂ of varying concentrations in 100 nM Tris-HCl buffer (pH 6.4).

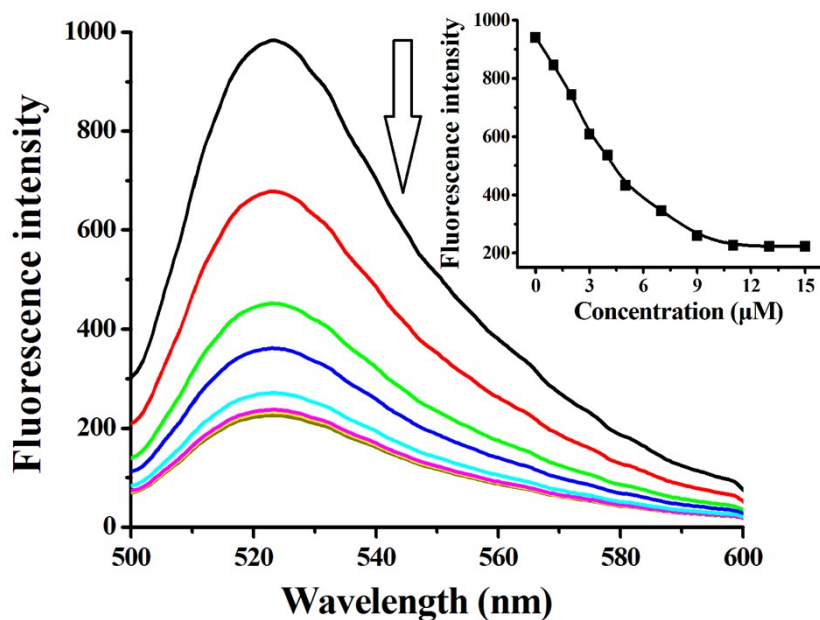


Fig. S10 Fluorescence spectra of P-DNA (50 nM) incubated with compound **1** of varying concentrations in 100 nM Tris-HCl buffer (pH 8.0) at room temperature. Inset: plot of the fluorescence intensity at 518 nm *versus* the concentrations of compound **1**.

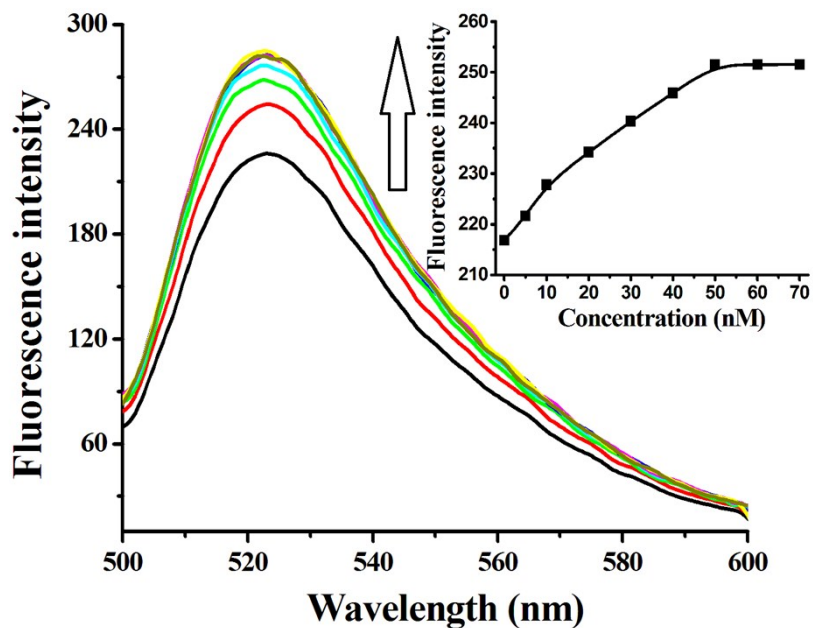


Fig. S11 Fluorescence spectra of the P-DNA@1 system (50 nM/13 μ M) incubated with T_0 of varying concentrations in 100 nM Tris-HCl buffer (pH 8.0) at room temperature. Inset: plot of the fluorescence intensity at 518 nm *versus* the concentrations of T_0 .

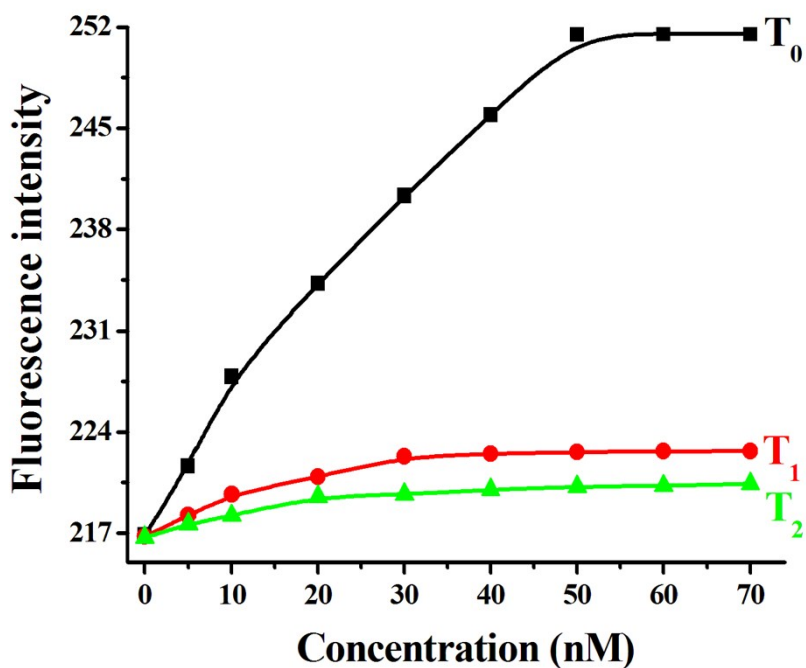


Fig. S12 Fluorescence recovery efficiency (518 nm) of P-DNA@1 system (50 nM/13 μ M) by T_0 , T_1 and T_2 of varying concentrations in 100 nM Tris-HCl buffer (pH 8.0).